ELSEVIER

Journal of Nuclear Materials 271&272 (1999) 128–132

journal of nuclear materials

The mechanical properties of 590 MeV proton irradiated iron

Y. Chen, P. Spätig, M. Victoria *

EPFL-CRPP Fusion Technology Materials, 5232 Villigen PSI, Switzerland

Abstract

The mechanical properties of 590 MeV proton irradiated pure α-iron have been investigated after irradiation at 320, 420 and 520 K to doses between 10^{-5} and 10^{-1} dpa. For comparison, corresponding tests were carried out on unirradiated iron specimens. Radiation hardening is observed at doses above 10^{-3} dpa for all irradiation temperatures and a $(\text{dose})^{1/4}$ dependence is found after irradiations at 320 K. It is shown that the irradiation suppresses the dynamic strain ageing observed in the unirradiated iron. The systematic observation of intergranular cracking in the specimens irradiated to doses of 10^{-3} dpa or larger is discussed in terms of dislocation channeling.

1. Introduction

Much of the early work since the initial observations of radiation hardening [1] and defect microstructures resulting from neutron irradiation [2] in α-iron has been reviewed by Little [3], who pointed out the following mean features of the hardening: a $(\phi t)^{1/2}$ dose dependence, a damage saturation dose of $\sim 10^{21}$ n cm^{-2} ($E > 0.1$ MeV) in pure iron and a strong effect of interstitial impurities. The defect structure after irradiation at reactor ambient temperature consists of small clusters or loops, probably interstitial in character. These observations have been confirmed more recently [4], after irradiation at higher temperatures (563 K) in both reactor and the RTNS II 14 MeV neutron source. Radiation softening has also been observed after irradiations at liquid helium temperatures and the annealing of this damage provides further indications of the interstitial nature of the irradiated damage microstructure [5–7].

The present investigation is part of a research program aiming at studying the possible effects of high energy recoils on the dose dependence and of microstructure and mechanical properties of pure metals and model alloys. These investigations are important for fusion materials because the recoil spectra of fusion neutrons has a mean energy much higher than that of fission reactor neutrons, which are the main irradiation media used at present, no intense 14 MeV neutron source being available. The PIREX [8] irradiation facility, with a beam of 590 MeV protons, is used for this purpose. The recoil spectra for protons of this energy has a maximum around 2–3 MeV in Fe [9]. It has already been shown that in fcc pure metals irradiated at 320 K, no difference is found in the microstructures and tensile properties between the materials irradiated in PIREX and those obtained after fission or fusion neutron irradiations [10].

2. Materials and techniques

Foils, 250 μm thick, of 99.99% pure iron were obtained from Goodfellow Cambridge. The main impurities, according to the nominal analysis provided by the supplier are B, Cr, Co, Cu, Ge, Mn, Ni and Si to a total of 100 wt. ppm and in addition 6.5 wt. ppm P and 3.8 wt. ppm S. No analysis of N was provided. The foils were annealed for 60 min at 923 K under vacuum to obtain a grain size of 30 μm. Flat microtensile specimens, with a 8 mm gage length 2.5 mm wide, were spark-cut from the annealed foil. The specimens were finally lightly electropolished before testing or irradiation. Tensile testing was performed in a screw drive Schenck testing machine, at a constant crosshead velocity of 20 μm min^{-1}. Tests at room temperature were performed in air or in vacuum,

* Corresponding author. Fax: +41-56 310 4529; e-mail: victoria@psi.ch.

0022-3115/99/$ – see front matter
PII: S0022-3115(98)00702-8

while all tests at higher temperatures, up to 623 K, were performed in vacuum only. Stress relaxations were systematically performed during tensile testing in order to obtain values of the activation volume of the deformation mechanism.

Irradiations were performed in the PIREX [8] facility installed in a beam line of the 590 MeV proton accelerator at the Paul Scherrer Institute in Switzerland, at an average damage rate of 1.3×10^{-6} dpa s^{-1}. The irradiation matrix included doses from 10^{-5} to 10^{-1} dpa at temperatures between 320 and 520 K.

3. Experimental results

3.1. Tensile tests

The microtensile specimens used in the present measurements have been shown to represent well the bulk tensile properties when the grain size is of the order of 30–50 μm. Only the total uniform elongation is smaller than that found in DIN type specimens [11].

Results from tensile testing at different temperatures of the unirradiated iron are shown in Fig. 1(a). The lower yield strength at 423 K is comparable to that measured at 295 K, but the work hardening is much higher. At higher deformation temperatures both the yield strength and the work hardening decrease systematically, but the work hardening becomes lower than that obtained after room temperature testing only in the test at 623 K. Serrations in the flow stress are observed at all testing temperatures above room temperature and they are specially marked in the test at 423 K. The lower yield stress, measured in every case after the initial yield point, is plotted as a function of the test temperature in Fig. 1(b).

The tensile behaviour at room temperature with dose after irradiations at 320 K is shown in Fig. 2(a). No hardening is observed below 10^{-5} dpa and the corresponding work hardening is actually lower than that of the unirradiated specimen. The strain associated with the yield region (Luders band propagation) increases with dose and probably accounts for the total deformation at 8×10^{-2} dpa, where practically no work hardening is observed. This is more clearly seen in the

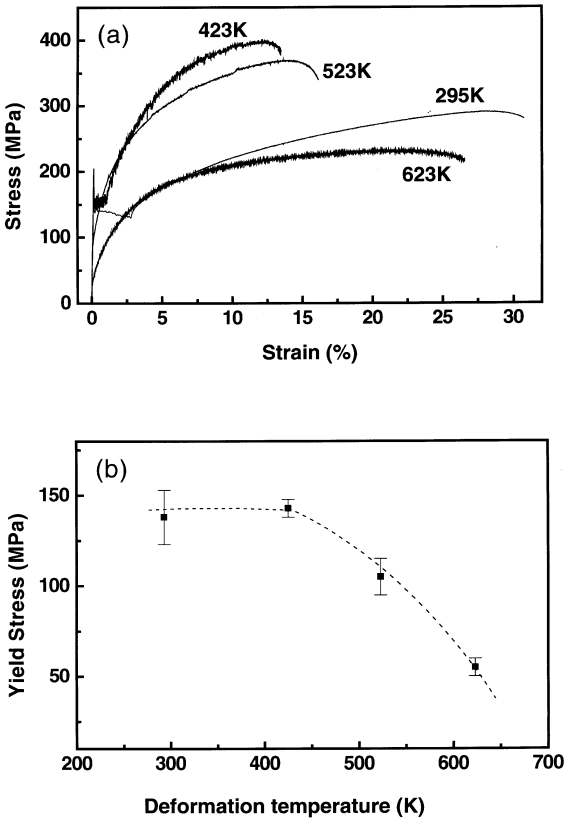

Fig. 1. (a) Tensile behaviour of α-iron at different temperatures. (b) Variation of the lower yield strength with temperature.

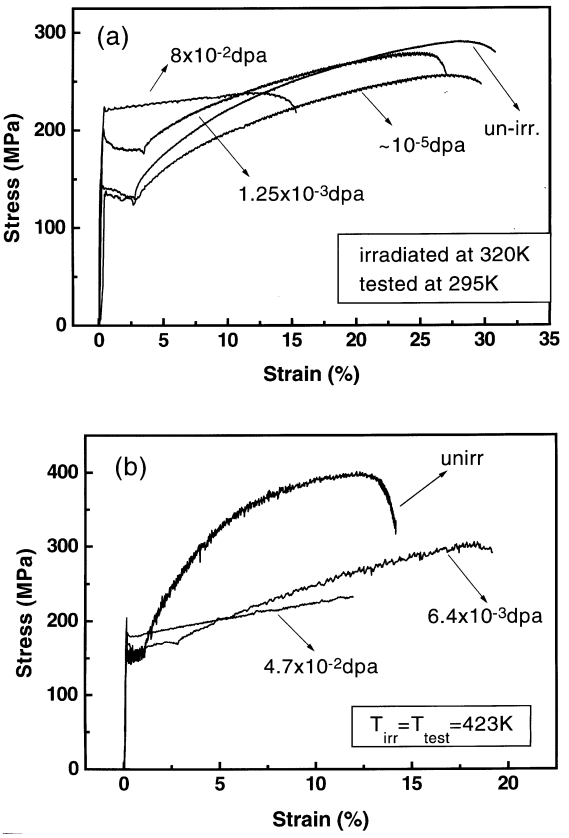

Fig. 2. Tensile behaviour of iron irradiated to different doses: (a) tested at room temperature; (b) tested at the irradiation temperature.

dose dependence at 423 K, shown in Fig. 2(b). The work hardening is almost linear and lower as the dose increases. Simultaneously, the serrations in the tensile curve disappear.

The dose dependence of the irradiation hardening $\Delta\sigma = \sigma_{\text{irr}} - \sigma_{\text{unirr}}$ is plotted in Fig. 3. The data is not sufficient for a precise determination, but the present data fits well a $(\text{dose})^{1/4}$ dependence after irradiations at 320 K. In the same figure, the effect of irradiation temperature on the dose dependence is also shown. The value $\Delta\sigma_T = \sigma^{\text{irr}}_{T\text{test}=T_{\text{irr}}} - \sigma^{\text{unirr}}_{T_{\text{irr}}}$ is plotted in this case, using the values corresponding to the lower yield strength. Again, the data set can only provide a trend showing the same $(\text{dose})^{1/4}$ dependence as for the lower irradiation temperature.

As for the dependence of the room temperature lower yield stress with irradiation temperature, values for two doses are plotted in Fig. 4. The yield stress decreases with irradiation temperature, at a comparable rate for both dose levels.

3.2. The activation volume

Apparent activation volumes V_{a} were obtained from stress relaxations along the tensile curve, according to the relation [12,13]

$$\Delta\sigma_{\text{r}} = \frac{kT}{V_{\text{a}}} \ln\left(\frac{t}{C} + 1\right),$$

where

$$C = \frac{MkT}{\dot{\varepsilon}_{\text{r}} V_{\text{a}}}.$$

M is a constant determined from the stiffness of the testing machine and t is the relaxation time.

Because of the difficulty in establishing the correct stress level in strongly serrated tensile curves, the values of the activation volume show a larger dispersion than is normally observed, but trends can be clearly detected. As the serrations tend to disappear at higher stresses, a corresponding improvement in the scatter of the activation volumes is seen.

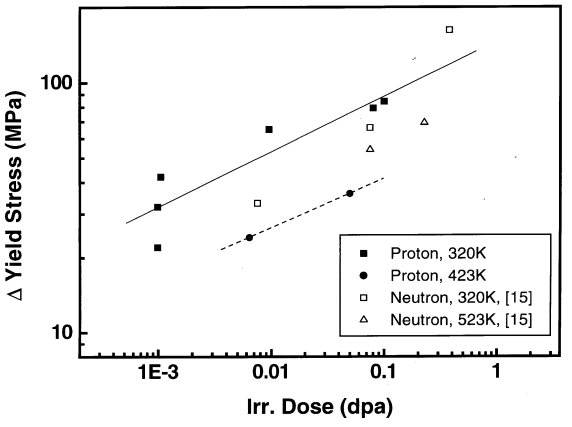

Fig. 3. Irradiation dose dependence of the yield strength of iron. The neutron irradiation on the same batch of Fe is from Ref. [15].

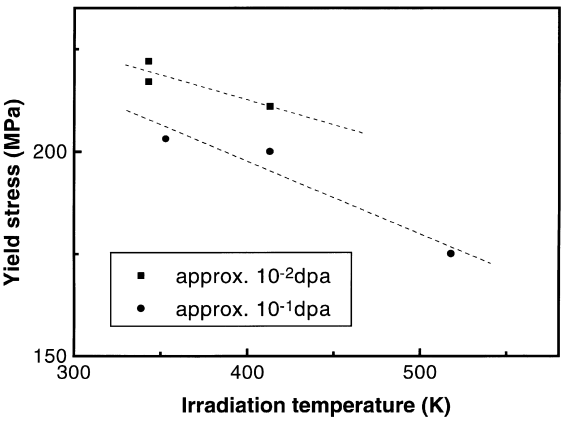

Fig. 4. Dependence of the yield strength with temperature at two different doses.

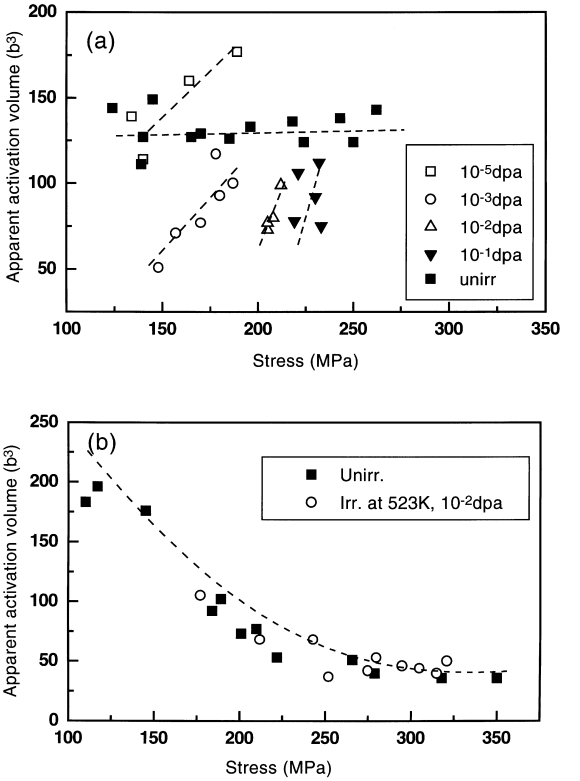

Fig. 5. Stress dependence of the apparent activation volume. (a) the effect of irradiation dose at room temperature, (b) the effect of irradiation at $T_{\text{irr}} = 523$ K.

The activation volume values for three different doses at 320 K and those of the unirradiated specimen are shown in Fig. 5(a), as a function of stress. Although the range of stress covered is not large enough, it can be seen that, except for the values obtained after 10^{-5} dpa, where no radiation hardening was found, the value of the activation volume of the irradiated specimens increase with stress towards the unirradiated asymptotic value of $125b^3$, where b is the Burgers vector. For higher temperature irradiations, the behaviour of the activation volume as a function of stress for both the irradiated and unirradiated material coincide, see Fig. 5(b). The asymptotic value of V_a at high stresses is $\sim 40\ b^3$.

3.3. Surface observations

Scanning microscope observations were performed on the deformed specimens. Typical observations after room temperature deformation are shown in Fig. 6. While the unirradiated specimen, Fig. 6(a), shows only a microcrack starting to develop in the neck region, the irradiated specimen ($T_{irr} = 320$ K, 10^{-3} dpa) shows a distribution of microcracks over the gage length, Fig. 6(b). As can be seen in Fig. 6(c) and Fig. 6(d), these are produced mainly at grain boundaries and at triple points. In surface observations at different strains in an interrupted tensile test, the microcracks are observed already after 12% elongation at this particular dose and temperature.

4. Discussion

The presence of a large yield point and serrated yielding in the tensile curve at 423 K is an indication that a mechanism of dynamic strain ageing (DSA) is operative, which is usually associated with the presence of interstitial impurities. Although C is below the ppm level, N was not analysed. It is also possible that the specimens could have picked up N during the vacuum anneal. It was very early recognised [14] that these extrinsic interstitials can combine with the irradiation produced defects, forming stable complexes, the creation of which reduces then the net concentration of interstitials in the lattice. Such mechanism implies that as the irradiation dose is increased, the DSA will disappear. This is readily observed in the specimens irradiated at 423 K after 10^{-2} dpa.

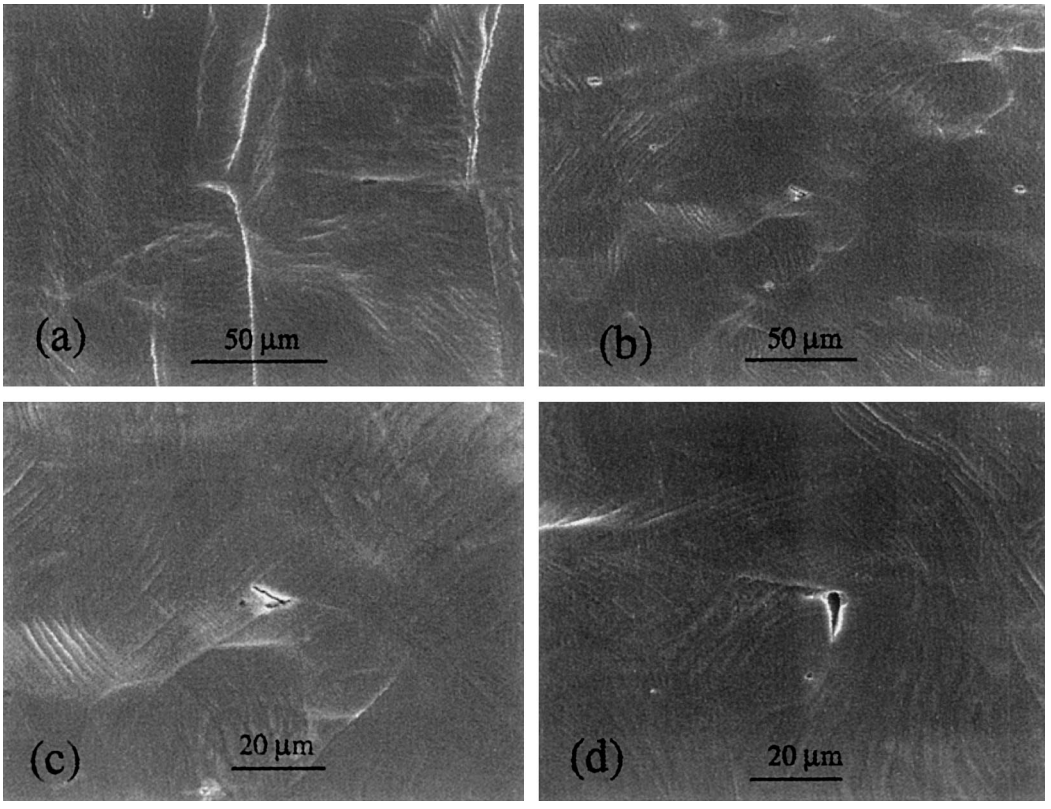

Fig. 6. (a) cracking at the neck in the unirradiated specimen; (b), (c) and (d) intergranular cracking in the irradiated specimen, at different magnifications. 10^{-3} dpa at $T_{irr} = 320$ K.

The observed irradiation hardening has been correlated in previous investigations with the presence of small clusters and loops of interstitial character, i.e. see Ref. [4]. No electron microscopy observations have been performed as yet in the proton irradiated iron, so there is no information on the characteristics of the proton irradiated microstructure. From the present results it can be inferred that only a very small density of such defects is produced after proton irradiation to 10^{-5} dpa at 320 K, since no hardening has been observed under these conditions.

A comparison of the results of the present investigation can be made to those of the neutron irradiated iron samples produced out of the same batch as the ones used here. The dose dependence results from this investigation [15] have been included in Fig. 3 and although the scatter is large, the trends are comparable after $T_{irr} = 320$ K. At higher irradiation temperatures, there are only two values for protons and two for neutron irradiation but neutrons seem to be more effective than protons in terms of hardening.

The trend of the activation volume of the irradiated material is consistent with the destruction of irradiation induced obstacles by the moving dislocation. After some amount of deformation the obstacle density decreases to the point were other obstacles (i.e. those pre-existing from the unirradiated state) control the deformation. It is unclear at this point what is the mechanism operative in the very low dose case (10^{-5} dpa), were the irradiation dose is not sufficient to produce a hardening defect microstructure

Although the activation volume data set at lower irradiation temperatures is still incomplete, it is clear from the strain/stress dependence of V_a after $T_{irr} = 523$ K that probably the operative rate controlling deformation mechanism is the same for the unirradiated and irradiated specimen.

Finally, the observed cracking localised at grain boundaries is believed to be associated with dislocation channeling: the dislocations sweep the irradiation produced defects as they move, so that it is easier for successive dislocation to glide in the same slip plane. This process leads to localised deformation by the formation of slip bands, in which several percent shear is accumulated. The localisation of such shear band at the grain boundary leads to the formation of the microcrack. The formation of dislocation channels has been observed after neutron irradiation [15].

5. Conclusions

(i) Radiation hardening is observed as a result of irradiation with 590 MeV protons at doses of 10^{-3} dpa or greater, in the 320–523 K temperature range.

(ii) The presence of DSA which is suppressed by irradiation to 6.4×10^{-3} dpa, is probably due to the presence of N.

(ii) A $(\text{dose})^{1/4}$ dependence is found at $T_{irr} = 320$ K, which is comparable to that obtained after neutron irradiation of iron of the same batch. At higher irradiation temperatures, hardening by neutron irradiation seems to be more effective.

(iv) Intergranular cracking has been systematically found in the irradiated iron at doses of 10^{-3} or higher. It is believed that this is an intrinsic mechanism of irradiated materials that deform by the dislocation channeling mode. Careful evaluation is needed of its effects on the small size specimens that are planned to be used in future fusion neutron sources.

Acknowledgements

The present research has been funded by the Swiss National Research Fund and the EU Fusion Technology Program.

References

[1] G.P. Seidel, Phys. Stat. Sol. 25 (1968) 175.
[2] B.L. Eyre, Philos. Mag. 7 (1962) 2107.
[3] E.A. Little, Int. Met. Rev. 21 (1976) 25.
[4] A. Okada, T. Yasujima, T. Yoshiie, I. Ishida M. Kiritani, J. Nucl. Mater. 179–181 (1991).
[5] P. Groth, F. Vanoni, P. Moser, in: R.J. Arsenault (Ed.), Proceedings of the International Conference On Defects and Defect clusters in bcc Metals and Alloys, AIME, 1963, p. 19.
[6] K. Kitajima, H. Abe, Y. Ono, E. Kuramoto, S. Takamura, J. Nucl. Mater. 108 (1982) 436.
[7] H. Matsui, H. Shimidzu, S. Takehana, M.W. Guinan, J. Nucl. Mater. 155–157 (1988) 1169.
[8] P. Marmy, M. Daum, D. Gavillet, S. Green, W.V. Green, F. Hegedus, S. Proennecke, U. Rohrer, U. Stiefel, M. Victoria, NIM B 47 (1990) 37.
[9] M. Victoria, M. Alurralde, A. Caro, A. Horsewell, S. Proennecke, Mater. Sci. Forum 97&98 (1992) 541.
[10] Y. Dai, M. Victoria, in: I.A. Robinson, G.S. Was, L.W. Hobbs, T. Diaz de la Rubia (Eds.), Proceedings of the Symposium on Microstructure Evolution During Irradiation, MRS 439, 1996, p. 319; see also Y. Dai, Thesis N^0 1388, Ecole Polytechnique Federale de Lausanne, 1995.
[11] P. Spätig, R. Schäublin, S. Gyger, M. Victoria, J. Nucl. mater. 258–263 (1998) 1345.
[12] F. Guiu, P.L. Pratt, Phys. Stat. Sol. 6 (1964) 111.
[13] L.P. Kubin, Philos. Mag. 30 (1974) 705.
[14] G.P. Seidel, Rad. Effects 1 (1969) 177.
[15] B.N. Singh et al., these Proceedings.